This document is the Accepted Manuscript version of a Published Work that appeared in final form in Colloids and Surfaces B: Biointerfaces. To access the final edited and published work see 10.1016/j.colsurfb.2019.04.030.

Nanotechnology-based formulations for resveratrol delivery: Effects on resveratrol *in vivo* bioavailability and bioactivity

Ana Cláudia Santos[a,b,*,1], Irina Pereira[a,b,1], Miguel Pereira-Silva[a], Laura Ferreira[a], Mariana Caldas[a], Mar Collado-González[c], Mariana Magalhães[a,b], Ana Figueiras[a,b], António J. Ribeiro[a,d], Francisco Veiga[a,b]

[a] Department of Pharmaceutical Technology, Faculty of Pharmacy, University of Coimbra, Coimbra, Portugal
[b] REQUIMTE/LAQV, Group of Pharmaceutical Technology, Faculty of Pharmacy, University of Coimbra, Coimbra, Portugal
[c] School of Food Science and Nutrition, University of Leeds, Leeds, United Kingdom
[d] i3S, Group Genetics of Cognitive Dysfunction, IBMC, Porto, Portugal

ARTICLEINFO

Keywords:
Resveratrol
Nanotechnology
Nanocarriers
Nanoparticles
Nanoencapsulation
Nanoformulations
Bioavailability
Bioactivity
In vivo

ABSTRACT

Resveratrol (RES), also known as 3,5,4′-trihydroxystilbene, is a polyphenolic phytoalexin that has been widely researched in the past decade due to its recognized numerous biological activities. Despite the potential benefits of RES, its effective use is limited due to its poor solubility, photosensitivity and rapid metabolism, which strongly undermine RES bioavailability and bioactivity. Thereby, recently, nanotechnology appeared as a potential strategy to circumvent RES physicochemical and pharmacokinetics constrains. However, only few studies have addressed the crucial *in vivo* suitability of the developed delivery systems to improve RES efficacy. Facing this scenario, in the present review, it is intended to present and discuss the *in vivo* resveratrol bioavailability and bioactivity, following its encapsulation or conjugation in nanotechnology-based carriers, contemplating their pharmacokinetics effectiveness.

Abbreviations: ^{18}F FDG, ^{18}f-fluorodexoyglucose; Avi, avidin; AD, Alzheimer's disease; ALT, Alanine aminotransferase; AST, Aspartate aminotransferase; AUC, area under the concentration time-curve; $AUC_{0\rightarrow 24h}$, area under the concentration-time curve from time zero to 24 h; $AUC_{0\rightarrow 8h}$, area under the concentration-time curve from time zero to 8 h; $AUC_{0\rightarrow\infty}$, area under the concentration time-curve from time zero to infinity; $AUC_{0\rightarrow a}$, rea under the concentration time-curve from time zero to the last measurable drug concentration; Aβ, amyloid-β; Aβ1-42, amyloid-β1-42; Bio, biotin; BBB, blood-brain-barrier; BCS, biopharmaceutics classification system; BSA, bovine serum albumin; CAM, chick embryo chorioallantoic membrane; CD, cyclodextrin; Cl, clearance; C_{max}, maximum concentration in plasma; CMCS, carboxymethyl chitosan; CoQ10, coenzyme Q10; COX-2, cyclooxygenase-2; cPLA2, cytosolic phospholipases A2; CS, chitosan; CS/PCL, chitosan-polycaprolactone; DGG, deacetylated gellan gum; DMBA, 7,12-dimethylbenz[*a*]anthracene; EE, encapsulation efficiency; F188, poloxamer 188; FA, ferulic acid; GI, gastrointestinal; GSK-3β, glycogen synthase kinase-3β; HO-1, heme-oxygenase-1; HPMC, hydroxypropylmethylcellulose; HP-β-CD, hydroxypropyl β-cyclodextrin; HSA, human serum albumin; i.p.i, ntraperitoneal; i.v.i, ntravenous; ICD, irritant contact dermatitis; IL-12, interleukin 12; IL-1β, interleukin 1β; IL-6, interleukin 6; iNOS, nitric oxide synthase; JNK, c-Jun N-terminal kinase; *Ka*, absorption rate constant; LCT, long-chain triglyceride; LDL, low density lipoprotein; LNC, lipid-core nanocapsule; LPS, lipopolysaccharide; MMP, matrix metalloproteinase; MUC- 2, mucin-2; MUC-3, mucin-3; mPEG-PCL, methoxy polyethylene glycol-poly(ε-caprolactone); MRT, mean residence time; NPs, nanoparticles; PAM-Chol, cholesterol-conjugated polyamidoamine dendrimer (PAMAM); PBS, phosphate-buffered saline; PCL, poly(ε-caprolactone); pDNA, plasmid DNA; PEG, polyethylene glycol; PEG-PLA, polyethylene glycol-polylactic acid; PET/CT, positron emission tomography/computed tomography; PI, polydispersity index; PLGA, poly (lactic-co-glycolic acid); PVA, polyvinyl alcohol; PVP K17, polyvinylpyrrolidone 17 PF; RES, resveratrol; RGD, argi- nine–glycine–aspartate; RM-β-CD, randomly methylated β-cyclodextrin; ROS, reactive oxygen species; SL, soybean lecithin; SLN, solid lipid nanoparticle; SNEDS, self-nanoemulsifying drug delivery system; SPIP, single-pass intestinal perfusion; $t_{1/2}$, plasma half-life; Tem, temozolomide; Tf, transferrin; TFF3, trefoil factor 3; t_{max}, time to achieve the maximum concentration in plasma; TNBS, trinitrobenzene sulphonic acid; TNF-α, tumor necrosis factor-α; TPGS, D-α-tocopherol polyethylene glycol 400 succinate; TTAB, tetradecyl trimethyl ammonium bromide; ZP, zeta potential; α-TOH, α-tocopherol

* Corresponding author at: Department of Pharmaceutical Technology, Faculty of Pharmacy, University of Coimbra (FFUC), Pólo das Ciências da Saúde, Azinhaga de Santa Comba, 3000-548, Coimbra, Portugal.
E-mail address: acsantos@ff.uc.pt (A.C. Santos).

[1] Both authors contributed equally to this work.

https://doi.org/10.1016/j.colsurfb.2019.04.030

1. Introduction

The use of nanotechnology-based carriers to encapsulate bioactive natural products, such as polyphenols, provides many advantages in the protection against degradation; in the interaction with the biological environment; in the enhancement of absorption, bioavailability, retention time, and improvement of intracellular penetration; and in the controlled delivery of these bioactive molecules [1]. Micelles, liposomes and nanoparticles (NPs) have been developed as polyphenols delivery nanocarriers, evidencing marked improvements in the dissolution rate of these bioactive molecules, improving their bioavailability and absorption [2]. Besides, certain nanocarriers are able to resist to the undesired liver metabolism, contributing to a more slowly decrease of the concentration of polyphenols in plasma in comparison with the administration of free polyphenols [3]. As a result, nanotechnology is able of overcoming the *in vivo* limitations of polyphenols [4]. However, concerns related to the nanoencapsulation of polyphenols have been reported, due to the varying structures, solubility and fast oxidation under basic conditions [5]. It is, thereby, crucial to take into consideration these impairing alterations on the polyphenols molecules when designing the nanocarriers.

The biodistribution profile and efficacy of polyphenols *in vivo* differs depending upon the particle size, surface charge, derivatization of the nanostructures surface and additional biophysical properties [5]. Particle size is a key factor in the biodistribution of long-circulating nanocarriers considering physiological parameters, such as hepatic filtration, tissue extravasation, tissue diffusion and kidney extraction [6]. In fact, the particle size of the nanocarriers contributes in a meaningful way to the nanocarriers' pharmacokinetics, through the balance between their *in vivo* biodistribution and clearance [7]. In addition, this characteristic impacts on the internalization process of the nanocarriers [8], being recognized that a particle size up to 500 nm enables the internalization process by cells [9,10]. The surface properties of the nanocarriers constitute another crucial factor, since those affect and determine important parameters as solubility, stability, clearance and the interaction of the nanocarriers with the cellular environment [5]. The relevance of the surface properties has led to the use of different natural and synthetic polymers to increase the stability of the nanocarriers by steric and electrostatic mechanisms. The nanocarriers coating with high positively or negatively charged polymers or the use of steric stabilizing agents, as polyethylene glycol (PEG), decrease the interactions among the nanostructures, conferring colloidal stabilization. PEGylated nanocarriers showed a decrease in the opsonisation rate, as well as a reduction in the absorption by the reticuloendothelial system, longer circulation times and higher levels of accumulation in their targets than non-PEGylated ones [11]. Overall, targeting strategies, both passive and active, allow to overcome drug resistance and to minimize the systemic concentration of the bioactive molecule, subsequently reducing side effects and the treatment duration. Modifying the surface of the nanocarriers in order to change the physicochemical characteristics, in particular the hydrophobicity and the zeta potential (ZP) constitute different approaches of passive targeting. Moreover, the active targeting refers to the functionalization of the nanocarrier surface by the selective coupling of ligands, such as antibodies, proteins, small molecules and aptamers, which evidence the capacity of recognition by the target cells. Thus, the targeting moieties enable the increase of the selective cellular binding and internalization processes through receptor mediated endocytosis [5].

Resveratrol (RES) is a well-known and distinguished polyphenol to be encapsulated or conjugated with nanotechnology-based carriers. RES, also known as 3,4′,5-trihydroxy-*trans*-stilbene, is a polyphenolic phytoalexin, belonging to the group of stilbenes, which is frequently traced in the skin of red grapes [12]. In line with this reason, in the beginning of the 90 s, in the outbreak period of the "French Paradox", the presence of RES in red wine was enquiringly linked to the low incidence of coronary heart diseases among French people, whom, regardless the high-fat diet, are assiduous consumers of red wine [13,14]. Since then, RES has been considered by the scientific community as molecule of particular interest, and several reports have identified wide biological activities. RES biological activity is intimately related to its chemical structure, which enables the interaction with cellular receptors and enzymes [15]. In fact, RES effectively targets extracellular radical oxygen species (ROS) when administered orally, thereby being a powerful anti-oxidant [16]. Moreover, RES exhibits immunomodulator, anticancer, antihypertensive, anti-inflammatory, anti-platelet aggregation and cardioprotective activities [17–22]. Owing to such, RES may be used in the prevention and treatment of different diseases, particularly chronic diseases, such as cancer [23], neurodegenerative diseases, as *e.g.*, Alzheimer's [24], and metabolic diseases, as *e.g.*, diabetes [25].

The therapeutic properties of RES were promptly exploited by the pharmaceutical industry and different conventional oral dosage forms have been developed [26]. Nevertheless, the administration of RES in its free form has restricted the *in vivo* bioavailability of RES, mainly due to its physicochemical and pharmacokinetics challenging features. As a matter of fact, RES belongs to the class II of the Biopharmaceutics Classification System (BCS) being, therefore, poorly soluble in water [27,28]. Furthermore, RES exists in the form of two geometric isomers: *trans*-RES (*t*-RES) and *cis*-RES, being the isomerization triggered by light exposure [29,30]. The two isomers show different chemical structures and, therefore, distinct bioactivities (Fig. 1). Furthermore, in comparison to *cis*-RES, the *trans*- isomer is less photosensible, and, consequently, evidences superior stability [29,31]. However, this stability is influenced by the pH and temperature of the *t*-RES solution, *i.e.*, the stability of *t*-RES is higher in acidic pH [31,32] and at lower temperatures [32]. Besides the RES photoinstability, the bioactive molecule is prone to auto-oxidation, which hinders is application *in vitro* and *in vivo*, mostly due to the production of complex semiquinones, quinines and toxic phenantrenoids [29,31].

Concerning RES pharmacokinetics, after oral administration, RES is well absorbed in the intestine through passive diffusion. Once in the bloodstream, it can be absorbed in the liver by passive diffusion or receptor mediated transport. RES can be metabolized to form glucuronide-RES and sulphate-RES derivatives or it can be found as free RES attached in a non-covalent manner to proteins, such as albumin,

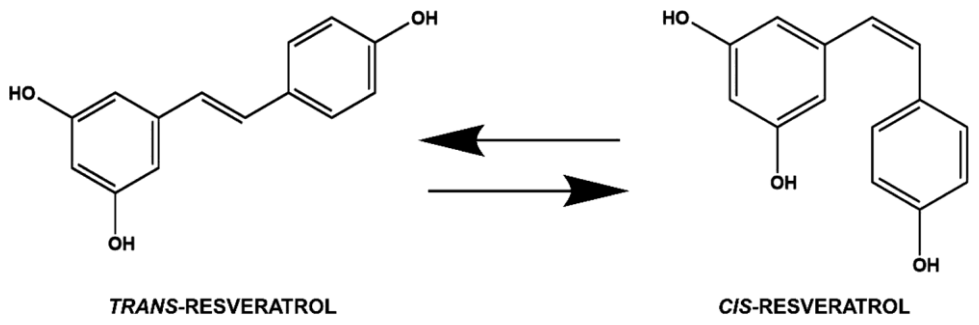

Fig. 1. Chemical structures of *trans*- and *cis*-resveratrol.

lipoproteins and, in particular, to a fraction of low density lipoproteins (LDLs) [33]. As a result, the free fraction of *t*-RES in plasma is very scarce, and it also presents a limiting short plasma half-life ($t_{1/2}$) [34]. Thereupon RES ingestion, two maximum peaks in RES plasmatic levels are obtained: one is found 30–60 min following ingestion, and a second peak is found after 6 h [35]. These findings suggest that an enteric recircularization of RES metabolites takes place. Henceforth, it has been proposed that an enzymatic hydrolysis of these metabolites occurs in the colon and in the enterocytes [33]. Considering this, the RES derived metabolites, if active, may constitute an additional source of RES [36].

RES reduced bioavailability is associated with several factors, including the poor water solubility, the isomerization, the auto-oxidation, and the rapid and extensive pre-systemic metabolism, which, consequently, strongly impairs RES therapeutic and disease-preventing activities. Therefore, the application of nanotechnology in the development of new carriers to properly deliver RES is highly desired to surpass the previously mentioned hurdles related to RES clinical administration and, ultimately, to enhance the health-promoting RES bioactive properties.

The present review highlights the recent *in vivo* studies regarding the bioavailability and bioactivity of nanotechnology-based carriers designed for RES delivery. This review critically exposes recent *in vivo* reports regarding the reported benefits, and also underlines some of the challenges related to the use of nanocarriers to deliver RES.

2. Methods of literature research

The PubMed free search engine from the Unites States National Library of Medicine and the Science Direct browser from Elsevier were used as searching tools to seek original research reports regarding nanocarriers-based formulations used to enhance the bioavailability and bioactivity of RES. The search was limited to the last 20 years, including publications from 1997 onwards. The following keywords were used: 'resveratrol', 'nanotechnology', 'nanocarriers', 'nanoparticles', 'nanoencapsulation', 'nanoencapsulated', 'nanoformulations', 'nanoemulsions', 'bioavailability', 'bioactivity', '*in vivo*'.

3. *In vivo* effects of resveratrol-loaded nanocarriers

Nanotechnology-based carriers have been extensively tested *in vitro* and *in vivo* to ascertain the effects on RES bioavailability and bioactivity. The next topic focuses on the *in vivo* effects that the administration of RES-loaded nanocarriers promote in RES bioavailability, and in anti-oxidant, anti-inflammatory, anticancer, neuroprotective, cardioprotective and wound-healing bioactivities (Fig. 2).

3.1. Bioavailability

The RES bioavailability effects after RES loading or conjugation with distinct types of nanotechnology-based carriers administered orally, intravenously, intranasally and intraperitoneally, which are discussed next, are summarized in Table 1.

The study of a RSV-loaded nanosuspension evidenced the capacity of this to alter the oral biovailability of RES, exhibiting a 3.3-fold greater maximum concentration in plasma (C_{max}) of RES and a 1.3-fold greater plasma exposure [*i.e.*, the area under the concentration time-curve from time zero to infinity ($AUC_{0\rightarrow\infty}$)] when compared to the C_{max} and $AUC_{0\rightarrow\infty}$ values of the reference formulation [37].

Polymeric nanocarriers based on poly (lactic-co-glycolic acid) (PLGA) were developed and orally administered in rats [7]. Subsequently, an enhancement of the rate and extent of RES bioavailability was observed. These RES-loaded PLGA NPs allowed for an 7.2-fold enhancement in the values of the absorption rate constant (K_a), as well as a 10.6-fold increase in $AUC_{0\rightarrow\infty}$ values when compared with free RES. Besides, the PLGA NPs showed a 2.8-fold increase RES concentrations in the liver. The *in situ* single-pass intestinal perfusion (SPIP) studies demonstrated that the use of PLGA NPs increased the absorption and permeability of RES through the Peyer's patches, protecting RES from the first-pass metabolism and gastrointestinal (GI) tract poor absorption, and, consequently, circumventing the enterohepatic recirculation [7]. PLGA was also used to produce D-α-PLGA:tocopherol polyethylene glycol 400 succinate (PLGA:TPGS) blend NPs (PLGA-BNPs) to prolong RES systemic circulation [38]. The single-emulsion solvent-evaporation technique was used to produce spherical RES-loaded RSV-PLGA-BNPs with *ca.* 175.5 nm. Tests to evaluate the haemolysis, erythrocyte membrane integrity and platelet aggregation were conducted and revealed that RES-PLGA-BNPs were non-toxic and hemacompatible, allowing the intravenous (i.v.) administration. In this work, pharmacokinetics studies were performed in Charles Foster rats following the i.v. administration of RSV-PLGA-BNPs (2.0 mg/kg) and free RES (solubilized using β-cyclodextrin (β-CD)). The area under the concentration time-curve (AUC) was approximately 15.9-fold higher than the AUC of the free RES suspension. Similarly, the $t_{1/2}$ and the mean residence time (MRT) were, respectively, *ca.* 18.1 and 12.5 times higher in comparison with the free RES suspension. The RES-PLGA-BNPs clearance (Cl) was inferior to that of free RES. Essentially, Vijayakumar and co-workers' pharmacokinetics findings demonstrated that TPGS avoids the NPs recognition by the reticuloendothelial system, prolonging RES $t_{1/2}$ and its systemic circulation, which, subsequently, enhances RES bioavailability. Moreover, in the same study, the biodistribution analysis showed highest accumulation of RES-PLGA-BNPs in the rats' brain (3.6 ± 0.5 μg/g for RES-PLGA-BNPs vs 0.8 ± 0.5 μg/g for free RES). Contrarily, the liver and spleen accumulation for RES-PLGA-BNPs was lower than that of free RES solution, pointing that PLGA-BNPs retarded the RES biotransformation process. Regarding these data, the brain targeting improvements of RES-PLGA-BNPs may assume particular importance in brain cancers therapy [38]. In a recent research, RES-loaded galactosylated PLGA NPs (RES-GNPs) were prepared by the solvent diffusion method [39]. The galactose ligand (*N*-oleoyl-D-galactosamine) anchored in the surface of the PLGA NPs was used to improve RES oral bioavailability. The authors assessed, in Sprague Dawley rats, the RES bioavailability after oral administration, by gavage, of a RES suspension (RES dispersed in a 0.3% carboxymethyl cellulose-sodium solution), RES-loaded PLGA NPs (without the galactose ligand, RES-NPs) and RES-GNPs. RES-GNPs evidenced the highest absolute bioavailability value (*ca.* 42.0%) when compared to RES-NPs (*ca.* 21.0%) and RES suspension (*ca.* 12.5%), suggesting that the polymeric NPs functionalized with galactose, with a particle size of 108.4 nm, a PI of 0.2, a ZP of -46.3 mV and an EE of 97.2%, may constitute a feasible strategy to enhance the oral bioavailability of RES. In fact, the RES-GNPs presented the highest AUC and C_{max} values (2-fold higher than that of RES-NPs) and the lowest time to achieve the maximum concentration in plasma (t_{max}). Furthermore, RES-GNPs improved RES intestinal permeability and transcellular uptake, which occured by ligand-receptor/transporter interaction [39].

Furthermore, recently, additional polymeric NPs loaded with RES and formed by TPGS, lecithin and PF-127 were orally administered to Sprague Dawley rats [40]. The doses administered were the equivalent to 20 mg/kg of RES. As a control, a free RES suspension was administered at the same doses. The C_{max} was 8.4 ± 1.4 μg/mL and the $AUC_{0\rightarrow\infty}$ was 43.4 ± 11.2 h.μg/mL. These C_{max} and $AUC_{0\rightarrow\infty}$ values were 2.2-fold and 3.5-fold higher, respectively, when compared with free RES. Besides, the MRT was 12.0 ± 2.0 h, which represents a 1.2-fold increase when compared to free RES MRT. Thus, an improvement on RES bioavailability was observed. This result was attributed to three reasons: (i) an upgrade in the NPs dissolution on the GI fluid; (ii) a raise in NPs bioadhesion; and, (iii) a NPs direct uptake across the intestinal barrier [40].

A similar increase in RES pharmacokinetics parameters were observed in RES-loaded Eudragit RL 100-tetradecyl trimethyl ammonium bromide (TTAB) NPs, which allowed an intensification of the values of K_a and an increase in the area under the concentration-time curve from

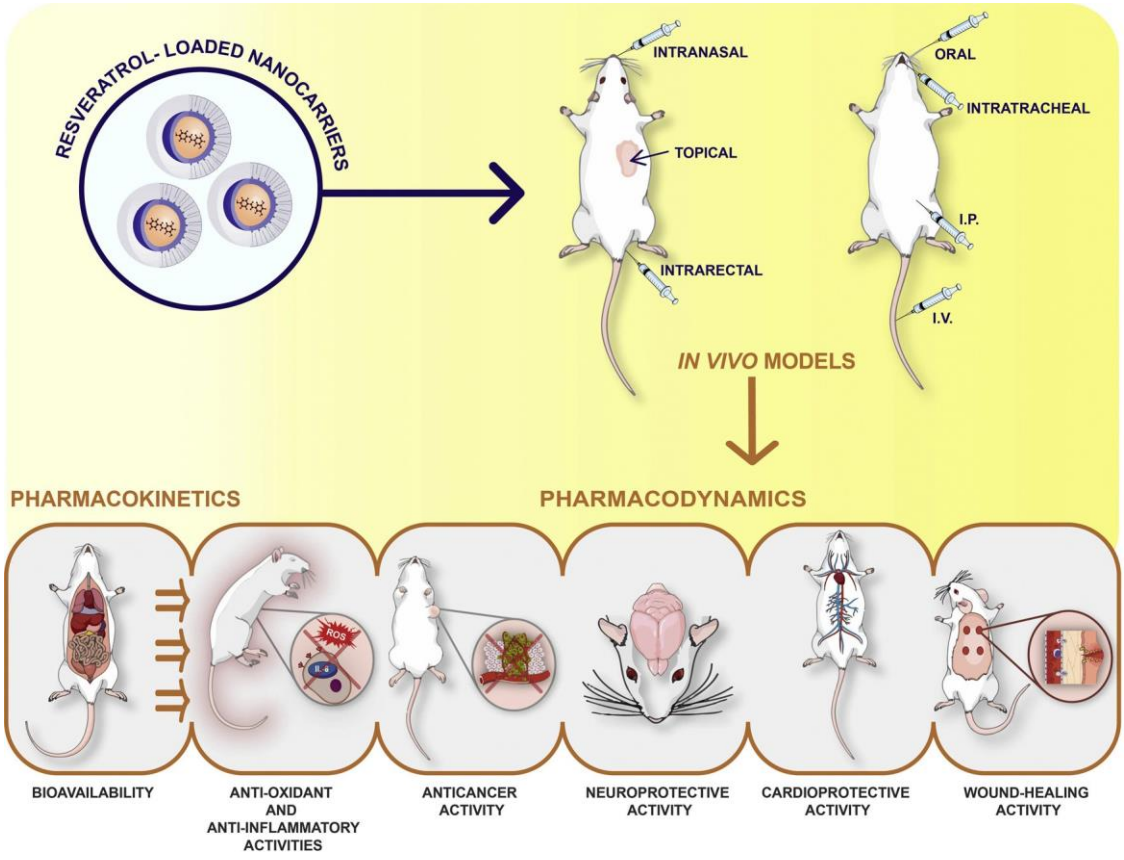

Fig. 2. RES bioavailability, anti-oxidant, anti-inflammatory, anticancer, neuroprotective, cardioprotective and wound-healing *in vivo* activities, promoted upon intranasal, topical, intrarectal, oral, intratracheal, intraperitoneal (i.p.) and intravenous (i.v.) administration of RES-loaded nanocarriers in rodents.

time zero to 24 h ($AUC_{0\rightarrow 24h}$) of 5.6-fold and 7.3-fold, respectively, indicating that, in comparison with free RES, the optimized NPs displayed a significant enhancement in the rate and extent of RES bioavailability [41]. NPs showed 4.1-fold rise in the values of RES concentrations in liver. In addition, *in situ* SPIP studies showed a remarkable enhancement of the absorption and permeability of NPs in relation to non-encapsulated RES [41].

NPs fabricated with a chitosan derivative, namely carboxymethyl chitosan (CMCS), have shown to improve RES anti-oxidant properties, as well as its aqueous solubility [42]. Zu and co-workers developed polymeric NPs based on CMCS to deliver RES (RES-CMCS NPs) by the oral route. The *in vitro* drug release of these NPs in simulated GI tract showed a RES release delay in relation to free RES. Compared with free RES, RES-CMCS NPs exhibited a rise in RES absorption and bioavailability in rats, as well as a prolonged duration of RES bioactivity in *in vivo* conditions. Concretely, the bioavailability of encapsulated RES was 3.5 times higher in comparison with the non-encapsulated RES [42]. Additionally, avidin (Avi) and biotin (Bio) modified chitosan (CS) NPs (Avi-Bio-CS-NPs) were used to load *t*-RES in order to test the effects on RES bioavailability, as well as the capacity of the RES-loaded NPs to target hepatic carcinoma cells in mice [43]. The Avi-Bio-CS-NPs displayed, in plasma, an area under the concentration time-curve from time zero to the last measurable drug concentration ($AUC_{0\rightarrow t}$) of 342.7 μg h/mL vs the 133 μg h/mL observed after i.v. administration of a free RES solution. The remaining pharmacokinetics parameters, particularly MRT and t_{max}, increased after the encapsulation of RES in Avi-Bio-CS-NPs, indicating an upgrade in the RES bioavailability [43].

A different type of biopolymer, gelatin, was used to encapsulate RES. RES-loaded gelatin NPs were administered intravenously and the results showed that, in contrast with free RES administration, RES serum levels were almost twice for RES-loaded gelatin NPs. In addition, the $t_{1/2}$ of NPs was substantially longer than that of free RES. Thus, the authors concluded that the loading of RES into gelatin NPs improved the pharmacokinetics parameters, and, consequently, the bioavailability of RES [44].

In a quite recent paper, Hao and co-workers synthesized an *in situ* gel containing RES nanosuspensions, and ionic-triggered deacetylated gellan gum (DGG) as a matrix [45]. The gel was designed to be intranasally administered in order to achieve RES nose-to-brain delivery in Kunming albino mice. This way, the DGG gel containing RES nanosuspensions was applied in the nasal mucus surface in one group of mice, whereas another group received it intravenously, through tail vein injection. RES plasma levels revealed that, contrarily to the i.v. injection, the intranasal administration of the gel containing RES nanosuspensions increased significantly the RES concentration in the brain. Indeed, the bioavailability of RES in the brain of the mice group that received the gel intranasally was 2.4 times higher than those who received it intravenously. In the brain, the C_{max} was 60.4 ± 35.2 ng/g, the area under the concentration-time curve from time zero to 8 h ($AUC_{0\rightarrow 8h}$) was 362.5 ± 169.0 h.ng/g, the MRT was 3.2 ± 0.7 h, the drug targeting efficiency was 458.5% and the drug direct transport effectiveness was 78.2%. In conclusion, the study of Hao and collaborators indicated that the *in situ* gel containing RES nanosuspensions enhanced RES bioavailability, further suggesting that the nose-to-brain route of administration is an alternative way to surpass the limitations associated with the blood-brain-barrier (BBB) [45]. The non-invasive and approachable intranasal route was seen as a secondary direct brain delivery pathway. Accordingly, it was recently exploited in the delivery of RES-loaded chitosan-coated lipid microparticles, which revealed significant improvements on RES bioavailability in the cerebrospinal fluid of Sprague Dawley rats [46].

A self-nano-emulsifying delivery system (SNEDS) composed by

Table 1
List of the most relevant *in vivo* studies concerning RES bioavailability upon oral, intranasal, i.v. and i.p. administration of different RES-loaded nanotechnology-based carriers.

Nanocarriers	*In vivo* model	Study	Via	RES Dose	Outcomes	Ref.
Nanosuspensions	Wistar rats	Pharmacokinetics in plasma	Oral	120.0 mg/kg	↑ bioavailability ($AUC_{0\rightarrow\infty}$ and C_{max} were, respectively, 1.3 and 3.4-fold greater^{*SUSP}); ↓ Cl (1.2-fold decrease^{*SUSP}); ↓ MRT (1.1-fold decrease^{*SUSP}); ↓ Vd (1.5-fold decrease^{*SUSP}).	[37]
Polymeric NPs (PLGA)	Wistar rats	Pharmacokinetics in plasma and *in vivo* biodistribution	Oral	20.0 mg/kg	↑ bioavailability ($AUC_{0\rightarrow\infty}$ was 10.6-fold greater^{*SUSP}; C_{max} was 1.2-fold greater^{*SUSP}); ↑ t_{max} (28.0-fold increase^{*SUSP}); ↑ absorption rate (K_a was 7.2-fold greater ^{*SUSP}); ↑ accumulation in the liver; ↓ elimination in brain, heart, lungs, kidneys and spleen.	[7]
		In situ intestinal perfusion (SPIP)	n.a.	0.2 mL/min (Perfusion rate)	↑ intestinal perfusion (8.5-fold increase ^{*SUSP}); ↑ magnitude of fraction absorbed (6.4-fold increase^{*SUSP}).	
Polymeric NPs (PLGA)	Charles Foster rats	Pharmacokinetics in plasma and *in vivo* biodistribution	i.v.	2.0 mg/kg	↑ bioavailability (AUC and $t_{1/2}$ were, respectively, 16.0 and 18.1-fold greater $^{*SOL(CD)}$); ↓ Cl (16.0-fold decrease$^{*SOL(CD)}$); ↑ MRT (12.5-fold increase$^{*SOL(CD)}$); ↑ Vd (1.2 -fold increase$^{*SOL(CD)}$); ↑ RES brain accumulation (4.5-fold increase$^{*SOL(CD)}$); ↓ accumulation in the liver, spleen and kidneys.	[38]
Galactosylated PLGA NPs (GNPs)	Sprague-Dawley rats	Pharmacokinetics in plasma	Oral	40.0 mg/kg	↑ bioavailability ($AUC_{0\rightarrow t}$ and C_{max} values were, respectively, 3.4-fold and 4.3-fold greater^{*SUSP}); ↓ t_{max} (3.0-fold increase^{*SUSP}); ↓ MRT (3.0-fold increase^{*SUSP}).	[39]
		In situ SPIP	n.a.	0.2 mL/min (Perfusion rate)	↑ intestinal permeability	
Polymeric NPs (TPGS)	Sprague-Dawley rats	Pharmacokinetics in plasma	Oral	20.0 mg/kg	↑ bioavailability ($AUC_{0\rightarrow\infty}$ and C_{max} were, respectively, 3.5 and 2.2-fold greater^{*SUSP}); ↑ MRT (1.2-fold increase^{*SUSP}).	[40]
Polymeric NPs (Eudragit RL 100)	Wistar rats	Pharmacokinetics and pharmacodynamics	Oral	20.0 mg/kg	↑ bioavailability($AUC_{0\rightarrow 24h}$ and C_{max} were, respectively, 7.3 and 1.3-fold greater$^{*FREE\ RES}$); ↓ t_{max} (12.0-fold increase$^{*FREE\ RES}$); ↑ absorption rate (K_a was 5.6-fold higher $^{*FREE\ RES}$); ↓ enterohepatic recirculation.	[41]
		In situ SPIP	n.a.	0.3 mL/min (Perfusion rate)	↑ absorption number (5.4-fold increase$^{*FREE\ RES}$);	
Polymeric NPs (CMCS)	Sprague-Dawley rats	Pharmacokinetics in plasma	Oral	50.0 mg/kg	↑ bioavailability (AUC and C_{max} were, respectively, 3.5 and 1.2-fold greater$^{*FREE\ RES}$); ↑ t_{max} (2.1-fold increase$^{*FREE\ RES}$);	[42]
Polymeric NPs (Avi-Bio-CS-NPs)	Kunming mice	Pharmacokinetics in plasma and liver	i.v.	0.3 mg/kg	↑ bioavailability in plasma (AUC was 2.6-fold greater^{*SOL}) ↑ t_{max} (25.0-fold increase^{*SOL}); ↑ MRT (4.5-fold increase^{*SOL}); ↑ bioavailability in the liver (AUC and C_{max} were, respectively, 2.5 and 1.7-fold greater^{*SOL}); liver targeting index = 2.5.	[43]
Polymeric NPs (Gelatin)	Swiss albino mice	Pharmacokinetics in plasma	i.v.	10.0 mg/kg	↑ bioavailability (2-fold increase$^{*FREE\ RES}$).	[44]
Polymeric Hydrogels (Nanosuspension-based *in situ* DGG gels)	Kunming mice	Pharmacokinetics in the brain	Intranasal	2.0 mg/kg	↑ bioavailability in the brain (2.88-fold increase in comparison to i.v. administration of the nanosuspensions); MRT = 3.4 ± 0.8 h; targeting efficiency = 458.2%; direct transport percentage = 78.2%.	[45]
Nanoemulsions (SNEDS)	Wistar rats	Pharmacokinetics in plasma	Oral	20.0 mg/kg	↑ bioavailability (AUC and C_{max} values were 4.3 and 2.3-fold greater^{*SUSP}); ↓ t_{max}; ↑ absorption rate; (K_a was 3.3-fold higher^{*SUSP}).	[28]
		In situ SPIP	n.a.	0.3 mL/min (Perfusion rate)	↑ absorption number (3.4-fold increase ^{*SUSP}); ↑ magnitude of fraction absorbed (2.4-fold increase^{*SUSP}).	
Nanoemulsions (SNEDS)	Wistar rats	Pharmacokinetics in plasma	Oral	20.0 mg/kg	↑ bioavailability (↑ AUC and ↑ C_{max}); ↓ t_{max};	[47]
		In situ SPIP	n.a.	0.3 mL/min (Perfusion rate)	↑ absorption number (3.8-fold increase$^{*FREE\ RES}$); ↑ magnitude of fraction absorbed (3.0-fold increase$^{*FREE\ RES}$); ↑ effective and wall permeability (3.9-fold and 5.2-fold, respectively, increase$^{*FREE\ RES}$).	
TPGS-coated Liposomes	Charles Foster rats		i.v.	2.0 mg/kg		[50]

(*continued on next page*)

Table 1 (*continued*)

Nanocarriers	*In vivo* model	Study	Via	RES Dose	Outcomes	Ref.
		Pharmacokinetics in plasma and *in vivo* biodistribution			↑ bioavailability (AUC and $t_{1/2}$ were, respectively, 29.9 and 29.6-fold greater$^{*SOL(CD)}$); ↓ Cl (33.0-fold decrease$^{*SOL(CD)}$); ↑ MRT (29.5-fold increase$^{*SOL(CD)}$); ↓ Vd (1.1-fold decrease$^{*SOL(CD)}$); ↑ RES brain accumulation (11.0-fold increase$^{*SOL(CD)}$); ↓ accumulation in the liver and kidneys.	
SLNs	Wistar rats	Pharmacokinetics in plasma	Oral	20.0 mg/kg	↑ bioavailability ($AUC_{0\rightarrow\infty}$, C_{max} and $t_{1/2}$ were, respectively, 8.0, 1.6 and 4.9-fold greater^{*SUSP}); ↑ t_{max} (4.0-fold increase^{*SUSP}); ↓ Cl (8.2-fold decrease^{*SUSP}); ↑ MRT (3.8-fold increase^{*SUSP}).	[51]
SLNs	Wistar rats	*In vivo* biodistribution	i.p.	5.0 mg/kg	↑ RES brain accumulation (4.9-fold increase$^{*FREE\ RES}$).	[52]
Protein-based NPs (Zein)	Wistar rats	Pharmacokinetics in plasma	Oral	15.0 mg/kg	↑ bioavailability (AUC and C_{max} were, respectively, 18.5 and 2.0-fold greater$^{*SOL(PEG)}$); ↑ t_{max} (8.2-fold increase$^{*SOL(PEG)}$).	[53]
Protein-based NPs (BSA)	Kunming mice	*In vivo* biodistribution	i.v.	1.5 mg/kg	↑ targeting efficiency; ↑ RES accumulation in the liver, kidney, heart, and ovaries; ↓ NPs concentration in the blood.	[55]
CDs (HP-β-CDs)	Sprague–Dawley rats	Pharmacokinetics in plasma	i.v.	5.0 mg/kg	No significant impact on the i.v. pharmacokinetics profile, even though it dramatically enhanced the aqueous solubility of RES; AUC = 236.1 ± 35.2 h.ng/mL; Cl = 21.6 ± 3.6 h.L/kg; Vd = 2.5 ± 0.7 L/kg.	[54]
				10.0 mg/kg	No significant impact on the i.v. pharmacokinetics profile, even though it dramatically enhanced the aqueous solubility of RES; AUC = 505.9 ± 68.1 h.ng/mL; Cl = 20.0 ± 2.6 h.L/kg ; Vd = 2.6 ± 0.4 L/kg.	
				25.0 mg/kg	No significant impact on the i.v. pharmacokinetics profile, even though it dramatically enhanced the aqueous solubility of RES; AUC = 2,196.2 ± 343.3 h.ng/mL; Cl = 11.6 ± 1.6 h.L/kg ; Vd = 2.2 ± 0.2 L/kg.	
CDs (RM-β-CDs)	Sprague–Dawley rats	Pharmacokinetics in plasma	Oral	15.0 mg/kg	AUC = 351.4 ± 17.2 h.ng/mL; ↑ C_{max}, but, it did not significantly increase RES oral bioavailability (C_{max} = 0.7 ± 0.05 ng/L); t_{max} = 0.083-0.25 h; F = 46.3 ± 9.9% (in contrast with the 46.4 ± 7.8% of the RES suspension in carboxymethyl cellulose).	
				25.0 mg/kg	AUC = 480.1 ± 24.2h.ng/mL; ↑ C_{max}, but, it did not significantly increase RES oral bioavailability (C_{max} = 0.9 ± 0.2 ng/L); t_{max} = 0.083-0.25 h; F = 38.0 ± 1.9% (in contrast with the 38.4 ± 9.0% of the RES suspension in carboxymethyl cellulose).	
				50.0 mg/kg	Did not significantly increase RES oral bioavailability; AUC = 1,009.0 ± 186.6 h.ng/mL; C_{max} = 1.8 ± 0.7 ng/L; t_{max} = 0.083-0.25 h; F = 39.9 ± 7.4% (in contrast with the 38.8 ± 2.0% of the RES suspension in carboxymethyl cellulose).	

Abbreviations: Avi-Bio-CS-NP - Avidin and biotin modified chitosan nanoparticle; AUC - Area under the concentration-time curve (plasma exposure); $AUC_{0\rightarrow24h}$ - Area under the concentration-time curve from time zero to 24 h; $AUC_{0\rightarrow\infty}$ - Area under the concentration time-curve from time zero to infinity; $AUC_{0\rightarrow8h}$ - Area under the concentration-time curve from time zero to 8 h; $AUC_{0\rightarrow t}$ - Area under the concentration time-curve from time zero to the last measurable drug concentration; BSA - Bovine serum albumin; Cl - Clearance rate; C_{max} - Peak plasma concentration; CMCS - Carboxymethyl chitosan; DGG - Deacetylated gellan gum; F - Relative bioavailability; HP-β-CD - Hydroxypropyl beta-cyclodextrin; i.p. – Intraperitoneal; i.v. – Intravenous; IVIVC - *In vitro*/*in vivo* correlation; K_a - Absorption rate constant; MRT - Mean residence time; n.a. - Not applicable; NP - Nanoparticle; PEG - Polyethylene glycol; PLGA - Poly (lactic-co-glycolic acid); RES - Resveratrol; RM-β-CD - Randomly methylated beta-cyclodextrin; SLN - Solid lipid nanoparticle; SNEDS - Self-nano-emulsifying drug delivery system; SPIP - Single-pass intestinal perfusion; $t_{1/2}$ - Plasma half-life; t_{max} - Time to achieve the maximum concentration; TPGS - D-α-tocopherol polyethylene glycol 400 succinate; *t*-RES - *Trans*-resveratrol; Vd - Volume of distribution; β-CD - β –cyclodextrin.

$^{*FREE\ RES}$ - Comparatively to free RES.

^{*SUSP} - Comparatively to free RES suspension.

^{*SOL} - Comparatively to free RES solution.

$^{*SOL(CD)}$ - Comparatively to free RES solubilized using β-CD.

$^{*SOL(PEG)}$ - Comparatively to free RSV solubilized in a PEG 400: water mixture.

long-chain triglycerides (LCTs), more precisely, Lauroglycol FCC (lipid) and the surfactants, Labrasol and Transcutol P, were used for *t*-RES delivery, demonstrating to enhance the pharmacokinetics *t*-RES values of K_a (3.3-fold), C_{max} (2.3-fold) and AUC (4.3-fold), in comparison with free *t*-RES, upon oral administration in rats [28]. These results indicated a significant enhancement in the rate and extent of bioavailability promoted by the *t*-RES-loaded nanoemulsions when compared with free *t*-RES. Alongside, *in situ* SPIP studies showed a remarkable enhancement in the absorptivity and permeability parameters of the nanoemulsion [28]. However, the previous nanoemulsion composed by Lauroglycol FCC, Labrasol and Transcutol P exhibited some limitations, namely the precipitation of *t*-RES upon long-term storage, shown by the presence of turbidity signs. Facing this problem, the same authors reformulated the nanoemulsion by adding hydroxypropylmethylcellulose (HPMC), a water-soluble polymer used as dispersing, emulsifying and thickening agent, that reduces the particles' sedimentation rate by increasing the viscocity of the aqueous medium, thereby, inhibiting agglomeration phenomena and the development of a sediment [47,48]. The resultant nanoformulation was evaluated by pharmacokinetics and *in situ* perfusion studies [47]. *In vitro* dilution of the HPMC-nanoemulsion resulted in a decelerated *t*-RES precipitation in comparison to the previous discussed formulation, where *t*-RES suffered rapid precipitation, yielding a low *t*-RES plasma concentration [28,47]. Pharmacokinetics studies indicated that the $AUC_{0\rightarrow 8h}$ of the HPMC-nanoemulstion evidenced a 1.3-fold increase in comparison to the previous nanoemulsion in the absence of the precipitation inhibitor. A significant improvement in the rate and extent of absorption was shown by *in situ* perfusion studies. Thus, the supersaturated nanoemulsion approach reinforced with HPMC effectively delivered *t*-RES, improving its oral bioavailability [47].

A pharmacokinetics evaluation of liposomes and nanoliposomes containing RES concluded that, in contrast to liposomes, the nanoliposomes (particle size inferior to 50 nm) significantly increased RES plasma concentrations [49]. The AUC evaluated for 10 h was found to be 2108.6 ± 61.0 ng.h/mL for liposomes, and 5823.0 ± 1016.3 ng.h/mL for nanoliposomes; the C_{max} was significantly different, being 396.9 ± 39.5 ng/mL for liposomes and 856.5 ± 112.4 ng/mL for nanoliposomes. In contrast, the t_{max} was greater for liposomes than for nanoliposomes, which proves that the nanoliposomes promoted a rapid RES absorption when compared to RES liposomes [49]. In Vijayakumar, *et al.* [50], the coating of RES-loaded liposomes (particle size of *ca.* 64.5 nm) with TPGS (RES-TPGS-liposomes) triggered positive effects on RES pharmacokinetics parameters. The RES-TPGS-liposomes were produced by the thin film hydration method using phosphatidylcholine and cholesterol as lipids. The optimal liposomal formulation evidenced a spherical shape and a high encapsulation efficiency (EE) of *ca.* 83.1%. The RES-TPGS-liposomes were i.v. administered (equivalent to 2 mg/kg of RES) in Charles Foster rats and evidenced improvements in the bioavailability of RES. The AUC, the $t_{1/2}$ and the MRT of RES-TPGS-liposomes were 29.9, 29.6 and 29.5-fold higher than free RES solubilized using β-CDs, respectively. Similarly, RES-TPGS-liposomes exhibited higher AUC, $t_{1/2}$ and MRT values than the RES-liposomes nanoformulation (*i.e.*, without the TPGS coating). RES-TPGS-liposomes revealed lower Cl values than free RES (33.1 times lower) and RES-liposomes (6.4 times lower). Thus, the pharmacokinetics data clearly demonstrated that TPGS-coated liposomes may constitute a feasible approach to enhance RES i.v. bioavailability [50]. Furthermore, in the same study, the tissue distribution analysis indicated that RES-TPGS-liposomes showed highest accumulation in the brain (8.9 ± 0.9 μg/g) in comparison with RES-liposomes (1.3 times higher) and free RES (11.0 times higher). In addition, RES-TPGS-liposomes presented lower values of liver and kidney accumulation than RES-liposomes and RES, suggesting that RES-TPGS-liposomes minimized RES biotransformation and elimination, thereby prolonging its systemic circulation, and, consequently, increasing RES brain biodistribution. In that sense, hemocompatible RES-TPGS-liposomes may be intravenously administered in order to passively target the brain [50].

Besides liposomes, RES was also encapsulated in lipid-based delivery systems with a solid matrix, *i.e.*, solid lipid nanoparticles (SLNs) [51,52]. In Pandita, *et al.* [51], the SLNs were produced by the solvent diffusion- solvent evaporation method using stearic acid as the lipid core, and a mixture Phospholipon® 90 G/poloxamer 188 as emulsifiers. The optimal RES-loaded SLNs formulation denoted a particle size of *ca.* 134.0 nm, a polydispersity index (PI) of 0.2, a ZP of -34.3 mV and an EE of approximately 88.9%. The oral administration of RES-loaded SLNs (20 mg/kg) in Wistar rats showed improvements in RES pharmacokinetics parameters. A higher plasmatic concentration of RES was attained for a longer period of time. The $t_{1/2}$ was 11.5 h for RES-loaded SLNs compared with 2.4 h for free RES. Accordingly, RES-loaded SLNs showed higher values of $AUC_{0\rightarrow\infty}$ and C_{max} in comparison with the one that received free RES. On the contrary, the Cl values were lower for RES-loaded SLNs. In Pandita and co-worker' study, SLNs demonstrated to improve the oral absorption and bioavailability of RES (the relative bioavailability was 8.0%). Overall, this lipid-based delivery system reduced RES enzymatic degradation and photodegradation, eliciting improvements on RES bioavailability [51]. In Jose, et al. [52] glyceryl behenate-based SLNs were prepared to deliver RES and target brain tissue. The *in vitro* release study showed that the RES-loaded SLNs followed a diffusion-controlled mechanism of RES release in phosphate-buffered saline (PBS) with a pH of 7.4. The *in vivo* biodistribution study, performed in Wistar rats, demonstrated that RES-loaded SLNs significantly increased the brain concentration of RES (17.3 ± 0.6 mg/g) as compared to free RES (3.5 ± 0.4 mg/g), suggesting SLNs as promising nanocarriers to increase RES bioavailability and bioactivity in neoplastic diseases located in the brain tissue. The RES-loaded SLNs accumulation in the brain occurred probably due to the reduction of liver uptake, that was promoted by the presence of Tween 80, an oral absorption enhancer, that was indicated to possibly mimicry the LDL receptors, facilitating BBB permeation [52].

In vivo pharmacokinetics studies were performed in male Wistar rats testing different RES-loaded zein NPs, a type of protein-based nanocarrier [53]. The bioavailability of the RES-loaded in zein NPs was 50.0% contrary to 2.6% obtained for RES and PEG400:water solution (19.2-fold upgrade in bioavailability). The upgrade in RES bioavailability may be particularly due to the hydrophobic character of zein NPs [53].

In contrast, the RES bioavailability in Sprague–Dawley rats did not suffer improvements after complexation with another natural starch-derived material from the cyclic oligosaccharides family, namely CDs [54]. Das et al. prepared RES inclusion complexes using hydroxypropyl-β-CDs (HP-β-CDs) and randomly methylated-β-CDs (RM-β-CDs), which were intravenously and orally administered, respectively. After i.v. administration of RES-HP-β-CDs, rapid elimination of RES was observed at all tested doses (5.0, 10.0, and 25.0 mg/kg); with non-linear elimination occurring at the highest dose. The authors hypothesized that, at high i.v. doses (25.0 mg/kg), the elimination process for RES may be saturated, which implies that dose escalation beyond its metabolic threshold may trigger the of increase RES plasmatic levels. Concomitantly, Das and co-workers observed that RES-RM-β-CDs significantly increased the C_{max} of orally administered RES, but no impact was detected on RES oral bioavailability, which remained unchanged among all investigated doses (15.0, 25.0, and 50.0 mg/kg). In line with these observations, the authors concluded that oral and i.v. administration of RSV inclusion complexes using CDs did not influence RES pharmacokinetics, attributing the verified increments in the absorption rate to the enhancement of the aqueous solubility of RES [54].

3.2. *In vivo bioactivities*

The improvements on RES anti-oxidant, anti-inflammatory, anticancer, neuroprotective, cardioprotective and wound-healing bioactivities after nanoencapsulation were detailed hereinafter. Table 2 outlines

Table 2
Results regarding RES *in vivo* bioactivity effects after conjugation or encapsulation in distinct types of RES-loaded nanotechnology-based carriers.

Bioactive molecule (s)	Nanocarrier	*In vivo* model	Target	Via	Dose	Treatment Duration/ Dosage	Main results	Ref.
Anti-oxidant and anti-inflammatory activities								
RES	Polymeric NPs (Eudragit E100 and PVA)	Acute hepatotoxicity-induced Wistar rats model	Liver	Oral	20.0 mg/kg	3 days/n.a.	↑ hepatoprotective effects, mediated by antioxidant and anti-inflammatory activities; ↓ ROS; ↓ lipid peroxidation in the hepatocyte membrane; ↓ AST and ALT.	[56]
RES	Nanoemulsions (Vitamin E and Sefsol 218®)	Haloperidol-induced Parkinson disease Wistar rats model	Brain	Intranasal	2.7 mg/day	n.a.	↑ anti-oxidant activity; ↓ degenerative neuronal injuries (eosinophilic lesions, vacuolation and shrinkage of nuclei).	[57]
RES	SLNs-based gel	New Zealand white rabbits DNCB-induced ICD BALB/c mice model	Skin Skin (ears)	Topical Topical	n.a. n.a.	n.a. n.a.	No irritation effects = safe. ↓ skin water content; ↓ ear swelling; ↓ epidermal thickness and edema.	[58]
RES	Protein-based NPs (Zein)	Endotoxic shock- induced C57BL/6 J mice model	Multi-target	Oral	15.0 mg/kg	7 days/once daily	↓ rectal temperature (slight); ↓ lethargy; ↓ TNF-α.	[53]
RES	Protein-based NPs (Silk fibroin)	TNBS-induced colitis Wistar rats model	Colon	Intrarectal	1.0 mg/rat	8 days/4 treatments	↓ edema; ↓ MPO activity; ↓ TNF-α, IL-1β, IL-6, and IL-12, CINC-1 and MCP-1 expression; ↓ ICAM-1 expression (adhesion molecule); ↑ MUC-2, MUC-3, TFF-3 and villin (improvement of the intestinal epithelium barrier function).	[59]
RES (Co-deliver with pHO-1)	Cholesterol-conjugated polyamidoamine dendrimer (PAMAM) (PAM-Chol micelles)	LPS-induced acute lung injury BALB/c mice model	Lungs	Intratracheal	n.a.	Single dose	↓ lung tissue edema and hemolysis; ↓ IL-1β; ↓ NF-kB activation.	[60]
Anticancer activity								
RES	Polymeric NPs (PEG-PLA)	CT26 colon cancer-bearing BALB/c nude mice	Colon cancer	i.v.	100.0 mg/kg	3 weeks/twice per week	↓ tumor growth; ↑ survival rate; ↓ ^{18}F FDG uptake.	[61]
RES	Polymeric NPs (Tf-modified PEG-PLA)	C6 glioma-bearing Sprague–Dawley rats	Brain cancer (glioma)	i.p.	15.0 mg/kg	n.a.	Accumulation of NPs in tumor tissue; ↓ tumor volume; ↑ survival rate.	[62]
RES (Co-deliver with Tem)	Polymeric NPs (mPEG-PCL)	U87 glioma-bearing nude mice	Brain cancer (glioma)	i.p.	10.0 mg/kg (RES dose) and 30.0 mg/kg (Tem dose)	n.a.	↓ tumor growth (slight); no weight loss.	[63]
RES	LNCs	C6 glioma-bearing Wistar rats	Brain cancer (glioma)	i.p.	5.0 mg/kg/day	10 days/once daily	↓ tumor size; ↓ intratumoral hemorrhaging; ↓ peritumoral edema; ↓ peripheric pseudopalisading;	[64]
RES	Nanocapsules (PCL)	B16F10 melanoma-bearing C57BL/6 J mice	Skin cancer (melanoma)	i.p.	5.0 mg/kg/day	10 days/once daily	↓ tumor volume; ↑ necrotic area and inflammatory infiltrate in the tumor; ↓ pulmonary hemorrhage; Prevented lung metastasis.	[65]
RES (Co-deliver with CoQ10)	Nanoemulsions (SNEDS, with α-TOH as excipient)	Breast cancer-bearing Sprague-Dawley rats (DMBA-induced)	Breast cancer	Oral	50.0 mg/kg (RES dose)	Single dose	↑ tumor latency; ↓ tumor volume; ↑ survival rate;	[66]

(*continued on next page*)

Table 2 (*continued*)

Bioactive molecule (s)	Nanocarrier	*In vivo* model	Target	Via	Dose	Treatment Duration/ Dosage	Main results	Ref.
							↓ angiogenic markers levels (MMPs, TNF-α and IL-6).	
RES	Protein-based NPs (BSA)	$SKOV_3$ ovarian cancer-bearing BALB nu/nu mice	Ovarian cancer	i.p.	50.0, 100.0 and 200.0 mg/kg	4 weeks/once per week	↓ tumor growth; ↑ tumor inhibition rate; ↑ apoptotic bodies; ↑ Cyto c, caspase-9, and caspase-3 proteins (in the higher dose).	[55]
RES	Protein-based NPs (HAS functionalized with RGD)	PANC-1 pancreatic cancer cells-bearing BALB/c nude mice	Pancreatic cancer	i.v.	10.0 mg/kg	35 days	↑ cancer targeting efficiency; ↓ tumor growth; No signs of tissue toxicity.	[67]
Neuroprotective activity								
RES	LNCs	Memory dysfunction Wistar rats model	Brain	i.p.	5.0 mg/kg/day	14 days/twice daily	↓ Aβ1-42-triggered memory impairment; ↓ synaptotoxicity; ↓ astrogliosis and microglial activation; ↓ JNK, GSK-3β activation; ↓ β-catenin phosphorylation; ↑ cytoplasmatic β-catenin levels.	[68]
Cardioprotective activity								
RES	Emulsion-liposome blends	Sprague-Dawley rats balloon injury model	Carotid arteries	i.p.	1.0 and 3.0 mg/kg	7 days before and 14 days after balloon injury	↓ neointimal area; ↓ neointimal area/medial area ratio; ↓ proliferation of arteries; ↓ restenosis.	[70]
Wound-healing activity								
RES (Co-deliver with FA)	Nanofibrous scaffolds (CS/PCL)	Albino Wistar rats	Skin wounds	Topical	n.a.	n.a.	↑ wound closure rate; no infections or allergies; thicker epidermis and more blood vessels; formation of hair follicles and sebaceous glands; ↑ tight collagen synthesis and deposition.	[71]

Abbreviations: ^{18}F FDG - ^{18}F-fluorodexoyglucose; ALT - Alanine aminotransferase; AST - Aspartate aminotransferase; Aβ1-42 - Amyloid-β (Aβ) 1–42; BSA - Bovine serum albumin; CINC-1 - Cytokine-induced neutrophil chemoattractant; CoQ10 - Coenzyme Q10; CS/PCL - Chitosan-polycaprolactone; Cyto *c* - Cytochrome *c*; DMBA - 7,12-dimethylbenz[*a*]anthracene; DNCB - Dinitrochlorobenzene; FA – Ferulic acid; GSK-3β – Glycogen synthase kinase-3β; HSA - Human serum albumin; i.p. - Intraperitoneal; i.v. - Intravenous; ICAM-1 - Intercellular Adhesion Molecule-1; ICD - Irritant contact dermatitis; IL-12 - Interleukin 12; IL-1β - Interleukin 1β; IL-6 - Interleukin 6; JNK - c-Jun N-terminal kinases; LNC - Lipid-core nanocapsule; MCP-1 - Monocyte chemoattractant protein-1; MMP - matrix metalloproteinase; mPEG-PCL - Methoxy polyethylene glycol-polycaprolactone; MPO - Myeloperoxidase; MUC-2 - Mucin 2; MUC-3 - Mucin 3; n.a. - Not applicable; PCL - Poly(ε-caprolactone); PEG-PLA - Polyethylene glycol-polylactic acid; pHO-1 - heme oxygenase-1 gene-inserted plasmid DNA; PVA - Polyvinyl alcohol; RES - Resveratrol; RGD - arginine–glycine–aspartate; ROS - Reactive oxygen species; SLN - Solid lipid nanoparticle; SNEDS - self-nanoemulsified delivery system; Tem - Temozolomide; Tf – Transferrin; TFF-3 - Trefoil factor 3; TNBS - Trinitrobenzene sulphonic acid; TNF-α - Tumor necrosis factor-α; *t*-RES - *Trans*-resveratrol; α-TOH- α-tocopherol.

the most significant outcomes that different RES-loaded nanotechnology-based carriers promote on RES bioactivities.

3.2.1. Anti-oxidant and anti-inflammatory activities

The use of RES-loaded nanocarriers has been remarkably reported in literature to increase the anti-oxidant and anti-inflammatory activity of this phytoalexin. Several works have already investigated RES-loaded NPs as a potential strategy to: (i) reduce RES hepatotoxicity; (ii) minimize neurodegenerative disorders symptoms; (iii) reduce anti-inflammatory processes; (iv) attenuate irritant contact dermatitis; (v) reduce endotoxic shock syndrome symptoms; (vi) treat inflammatory bowel disease; and, lastly, to (vii) treat acute lung injury.

Lee and co-workers have estimated the potential of Eudragit E100 and polyvinyl alcohol (PVA)-based polymeric NPs to improve the hepatoprotective effect of orally administered RES in rats with hepatotoxicity [56]. These polymeric NPs, in comparison with free RES administration, diminished liver function markers, namely aspartate aminotransferase (AST) and alanine aminotransferase (ALT), by decreasing hepatocyte death and ROS content in the liver tissue. In addition, RES-loaded polymeric NPs exerted their anti-oxidant and anti-inflammatory activities through the reduction of inflammatory cytokines, namely tumor necrosis factor-α (TNF-α) and interleukin 1β (IL-1β). Furthermore, the RES-loaded polymeric NPs reduced the levels of cyclooxygenase-2 (COX-2), nitric oxide synthase (iNOS), cytosolic phospholipase A2 (cPLA2), and caspase-3, thereby, preventing hepatocyte apoptosis. These RES-loaded polymeric NPs exerted, thus, a superior hepatoprotective effect than non-encapsulated RES, being suggested as a chronic liver disease preventive approach [56].

In another study, the intranasal administration of RES-loaded nanoemulsions composed of vitamin E and propylene glycol mono caprylic ester (Sefsol 218®), as the oil phase, has led to significant reduction of the degenerative neuronal injuries in haloperidol-induced Parkinson's disease rats. Such behavior was mainly attributed to the RES and vitamin E synergetic anti-oxidant activity combined with the nanoemulsions brain efficient targeting [57].

Shrotriya, et al. [58] have synthetized a RES-loaded SLNs-based gel for the treatment of irritant contact dermatitis (ICD). The RES-loaded SLNs-based gel was analyzed in ICD-induced BALB/c mice models to check the nanoformulation anti-inflammatory potential. The topical application of the nanoformulation reduced ear swelling and edema, improving the skin histology of ICD-induced mice. The incorporation of the RES-loaded SLN in the gel increased, thus, RES skin retention, contributing to the enhancement of its anti-inflammatory bioactivity [58].

Zein NPs, that belong to the protein-based NPs group, were loaded with RES, and tested in mice models of endotoxic shock syndrome (similar to septic shock syndrome) to determine the nanoencapsulation effects on the RES anti-inflammatory activity [53]. Lipopolysaccharide (LPS), a prototypical endotoxin that can directly activate the macrophages and induces the production of inflammatory cytokines, was administered intraperitoneally in C57BL/6 J mice. The daily oral administration of RES-loaded zein NPs, for a total time treatment period of 7 days, reduced the endotoxic signs, particularly hypothermia and lethargy, in the mice models of endotoxic shock syndrome. The symptoms improvement was attributed to the reduction of TNF-α levels triggered by RES-loaded zein NPs administration. Thus, in Penalva, *et al.* [53] study, zein NPs are suggested as nanocarriers with the potential to enhance the RES anti-inflammatory activity.

Furthermore, other type of protein-based NPs, produced mainly by silk fibroin, were intrarectally administered to Wistar rats bearing colitis (a trinitrobenzene sulphonic acid (TNBS) experimental model) [59]. This investigation has shown that the RES-loaded fibroin NPs elicited a significant inhibition of the expression of pro-inflammatory cytokines, such as TNF-α, IL-1β, interleukin 6 (IL-6) and interleukin 12 (IL-12), producing intestinal anti-inflammatory effects. In addition, RES-loaded fibroin NPs have also showed immunomodulatory properties owing to the macrophage activity promotion. Besides that, RES-loaded fibroin NPs increased expression of mucins 2 and 3 (MUC-2 and MUC-3), as well as the expression of proteins, such as the trefoil factor 3 (TFF3) and villin, enhancing the intestinal epithelial integrity. This research, conducted by Lozano-Perez and co-workers, suggested that RES-loaded fibroin NPs reduce the colitis symptoms in the mice models, constituting a more effective anti-inflammatory single therapy when compared with the glucocorticoid dexamethasone, the standard drug used for chronic human inflammatory bowel disease [59].

In a recent paper by Kim, et al. [60] cholesterol-conjugated polyamidoamine dendrimer (PAMAM) micelles (PAM-Chol micelles) were synthetized to co-deliver RES and the heme oxygenase-1 (*HO-1*) gene, which encodes an enzyme that generates by-products that are correlated with the activation of inflammatory pathways. The micelles were produced using the oil-in-water emulsion/solvent evaporation method. The hydrophobic nature of RES allowed its loading into the hydrophobic core of the PAM-Chol micelle, and the positive surface of the micelle enabled the formation of complexes with plasmid DNA (pDNA) inserted with the *HO-1* gene (pHO-1), thus, forming a multifunctional nanocarrier. The micellar complexes, with *ca.* 120.4 nm, were intratracheally administered to an LPS-induced acute lung injury mouse model. The findings of this study indicated that, even though the inhibition of NF-kB nuclear translocation was independent of the presence of pHO-1 and overall associated with RES, the pDNA/PAM-Chol/Res micellar complex effectively reduced lung tissue edema and hemolysis, as well as the levels of pro-inflammatory cytokines, namely IL-1β. Such occurred mechanisms conducted to an improved anti-inflammatory response when compared with the PAM-Chol/Res micelles (without the presence of pHO-1). The data obtained suggested that these micellar complexes might be an interesting nanoplatform to combine RES and gene therapies towards acute lung injury treatment *via* the intratracheal route.

3.2.2. Anticancer activity

The anticancer activity of RES has been distinguishably reported to improve upon nanoencapsulation. This promising ouput has been evidenced after the *in vivo* administration of RES-loaded polymer-based, lipid-based and protein-based NPs. The RES-loaded NPs were tested against colon, brain, skin, breast, ovarian and pancreatic cancers, and are exposed next.

Polyethylene glycol-polylactic acid (PEG-PLA) polymeric NPs loaded with RES were intravenously administered in CT26 colon cancer cells-bearing BALB/c nude mice [61]. The metabolic and anticancer effects of RES-loaded PEG-PLA NPs were investigated further. After a period of 21 days, the mice treated with RES-loaded PEG-PLA NPs presented a significant slower tumor growth curve in comparison with the mice treated with empty PEG-PLA NPs. The major discrepancy between the mice group that received the RES-loaded PEG-PLA NPs and the mice group treated with empty PEG-PLA NPs was observed 10 days after the first treatment (4^{th} dose). At that time, the empty PEG-PLA NPs treated mice group displayed a great increase in tumor size, whereas the tumor growth remained slow for the RES-loaded PEG-PLA NPs treated mice group. In the end of the treatment, the average survival rate was 18.0 ± 4.2 days for the RES-loaded PEG-PLA NPs group and 11.4 ± 8.0 days for the empty PEG-PLA NPs group. Moreover, the RES-loaded PEG-PLA NPs exhibited a tumor growth inhibition of 66.9%. Separately, but within the same study, Jung, et al. [61] conducted a micro positron emission tomography/computed tomography (PET/CT) study in which a tail injection of 7.4 MBq of ^{18}F-fluorodexoyglucose (^{18}F FDG) was administrated to the CT26 colon cancer cells-bearing BALB/c nude mice. RES is known to suppress cancer cell glucose metabolism and, Jung and co-workers, through the use of PET/CT, discovered that the administration of RES-loaded PEG-PLA NPs in mice reduced the tumor ^{18}F FDG uptake, pointing ^{18}F FDG as a potential RES-loaded NPs monitoring biomarker in colon cancers [61].

Modified PEG-PLA were also used to assess the antiglioma activity

of RES [62]. Concretely, the *in vivo* biodistribution and anticancer activity of transferrin (Tf)-modified PEG-PLA NPs conjugated with RES (Tf-PEG-PLA-RES) were investigated in C6 glioma-bearing rat models. The Tf receptor is expressed in brain capillaries, thereby, the functionalization of PEG-PLA NPs with the ligand for those receptors may enhance the NPs ability to target glioma cells, and consequently the NPs tumor biodistribution. In fact, the intraperitoneal (i.p.) administration of Tf-PEG-PLA-RES conjugates, in comparison with free RES, significantly decreased tumor volume and increased tumor accumulation, prolonging the survival of C6 glioma-bearing rats, offering a great potential as a targeted therapy for glioma [62]. Furthermore, additional polymeric NPs loaded with RES were developed to enhance the antiglioma effect of temozolomide (Tem), a chemotherapeutic drug used in brain cancer therapy, that poses some constrains due to the resurgent resistance of glioma cells [63]. The copolymer methoxy polyethylene glycol-poly(ε-caprolactone) (mPEG-PCL) was used in the obtainment of the RES-loaded NPs. The i.p. administration of RES (10 mg/kg) in U87 glioma-bearing nude mice *per se* did not produce any significant response comparatively to controls, whereas Tem (30 mg/kg dose) i.p. administration and Tem and RES co-administration displayed a small tumor growth inhibition. However, when the co-administration of Tem and RES was performed by using mPEG-PCL NPs, a significant increase in the anticancer effect was observed. It is crucial to further understand the mechanism of action of the co-administration of Tem and RES, nevertheless, the findings presented in Xu and co-workers study pointed out that the co-encapsulation of Tem and RES in polymeric NPs may be a potential dual approach against brain cancer resistance [63]. Similarly, the antiglioma effect of *t*-RES-loaded lipid-core nanocapsules (LNCs) was evaluated *in vivo* in C6 glioma-bearing Wistar rats [64]. The i.p. administration of *t*-RES-loaded LNCs, after a period of 10 days, showed a significant reduction in the tumor size. It was also observed a decrease of intratumoral hemorrhaging, peritumoral edema and peripheric pseudopalisading effects. These findings suggested that the *in vivo* benefits related with NPs are due to a decrease in plasma protein binding and a superior transportation of *t*-RES across the BBB, which is hyperpermeable in brain tumors [64].

RES-loaded oil core PCL nanocapsules produced by interfacial deposition of PCL were tested in B16F10 melanoma-bearing C57BL/6 J mice [65]. The i.p. administrationof RES-loaded PCL nanocapsules (5 mg/kg), for a period of 10 consecutive days, significantly reduced the tumor volume in the melanoma-induced mice model. Furthermore, in the histological evaluation, the authors observed that RES-loaded PCL nanocapsules increased the necrosis and inflammation in the tumor tissue, reduced the pulmonary hemorrhage and prevented lung metastasis. In the light of these results, the prophylactic and therapeutic potential of RES may be upgraded using nanocapsules as nanocarriers, constituting a thriving melanoma alternative therapy [65].

The cancer prophylactic potential of a RES and coenzyme Q10 (CoQ10) co-loaded SNEDS constituted by α-tocopherol (α-TOH) as an excipient (αTOH-RES-CoQ10-SNEDS) nanoformulation was tested in 7,12-dimethylbenz[*a*]anthracene (DMBA)-induced breast cancer rat model [66]. The αTOH-RES-CoQ10-SNEDSS was orally administered one day prior to the breast cancer induction in the animals. In Jain, et al. [66] study, the tumor latency was found to be higher in the α-TOH-RES-CoQ10-SNEDS pre-treated rats, since this group exhibited a tumorous lesion only at the tenth week (*ca.* 70 days after the last DMBA administration). Additionally, the pre-treatment with α-TOH-RES-CoQ10-SNEDS significantly reduced the tumor volume. A 100% survival rate and a reduction in the levels of angiogenesis markers (matrix metalloproteinases (MMPs), TNF-α and IL-6) were further observed in the animals pre-treated with α-TOH-RES-CoQ10-SNEDS. Henceforth, the co-administration of RES and CoQ10 resorting to the use of submicron SNEDS constituted by α-TOH as excipient may be deemed as a prospective prophylactic anticancer strategy [66].

RES-loaded NPs were also evaluated as an anticancer therapy for ovarian cancers [55]. Protein-based NPs composed of bovine serum albumin (BSA) were used to load RES, and this nanocarriers was examined on $SKOV_3$ human primary ovarian cancer-xenografted nude mice. The *in vivo* tissue distribution of RES was remarkably affected, namely by a greatly augmentation of RES concentration in the liver, kidney, heart, and mice ovaries. The administration of RES-loaded BSA NPs by the i.p. route significantly retarded the growth of $SKOV_3$ human primary ovarian cancer-xenografted nude mice from the third week onwards, and the inhibition rate was markedly higher than in mice treated with free RES (52.4% *vs.* 46.3%), without causing weight loss [55].

In a recent paper, Geng, et al. [67] produced RES-loaded human serum albumin (HSA) NPs conjugating arginine–glycine–aspartate (RGD) *via* PEG "bond" (HRP–RGD NPs) to target pancreatic cancer. The HRP–RGD NPs were i.v. administered to PNAC-1 pancreatic cancer-xenografted mice models. RES concentration in the tumor tissue for the mice group treated with HRP–RGD NPs was 3.0 and 8.1 times higher in comparison with the groups treated with HRP NPs (without RGD) and free RES, respectively. Such data indicated that the functionalization with RGD increased the HRP NPs cancer targeting efficiency. Moreover, after a 35-day treatment period, the HRP-RGD NPs efficiently suppressed the tumor growth with no signs of *in vivo* tissue toxicity, constituting a potential safe therapeutic approach for pancreatic cancer [67].

3.2.3. Neuroprotective activity

The age-related neurodegenerative Alzheimer's disease (AD) is known to cause cognitive impairment and memory loss due to the deposition of neurofibrillary tangles of hyperphosphorylated tau protein and amyloid-β (Aβ) peptide [68]. RES evidences anti-amyloidogenic properties, which are constrained by its confining physicochemical and pharmacokinetics characteristics [68,69]. Facing this scenario, Frozza, et al. [68] formulated LNCs in order to improve RES bioavailability and enhance RES concentrations in the brain. The RES-loaded LNCs were tested *in vivo* after an intracerebroventricular injection of Aβ1-42 (Aβ1-42) in Wistar rats. This treatment caused a significant impairment on learning memory ability, with a parallel significant decrease in hippocampal synaptophysin levels, together with a disruption in c-Jun N-terminal kinase (JNK) and glycogen synthase kinase-3β (GSK-3β) activation, and a destabilization of phosphorylated β-catenin levels. In this study, LNCs improved the RES neuroprotective effects through the prevention of synaptic dysfunction. In a 14 days period, the i.p. administration of a daily dose of 10 mg/kg of RES-loaded LNCs, in comparison with the administration of a free RES solution (dissolved in ethanol), was able to improve significantly the Aβ-induced memory impairment (treated rats displaying performances equivalent to their control counterparts). In the Aβ1-42-infused rats, LNCs increased the intracerebral concentrations of RES and reverted the synaptotoxicity, increasing the synaptophysin levels. Therefore, RES delivery by LNCs exhibited neuroprotective properties identified to lead to an innovative strategy to prevent or treat AD [68].

3.2.4. Cardioprotective activity

Reports have suggested that RES exhibits cardioprotective activity, being able to inhibit platelet aggregation and coagulation [70]. As a solution for RES poor water solubility, several authors have proposed the use of lipid emulsions and liposomes as carriers to deliver RES and potentiate its cardiovascular protection. Hung, et al. [70] developed a blend of lipid emulsions and liposomes with coconut oil, soybean lecithin (SL) and glycerol formal to deliver RES. The emulsion-liposome blends were tested in a Sprague-Dawley rat balloon injury model. In this model, an endothelial injury is produced in normal carotid arteries, which enables the observation of morphological changes. This test demonstrated that the use of RES in the different designed emulsion-liposome blends inhibited intimal hyperplasia, showing a considerable reduction in both neointimal area and the neointima/media ratio, thus diminishing the proliferation of arteries compared to the control.

Additionally, these findings suggested the ability of RES to treat restenosis, owing to the protection that the emulsion-liposome blends provided to the phytochemical. Regarding the toxicity of the nanoformulations, an erythrocyte hemolysis test was performed and the results indicated that the treatment with emulsion-liposome blends was less toxic than the treatment with non-encapsulated RES. These nanoformulations also prevented the accumulation of RES in kidneys and the liver, displaying only a minor lymphocyte aggregation in liver lobules. Overall, the evidences presented in Hung and co-workers study emphasized the potential therapeutic and preventive applications of RES emulsion-liposome blends in cardiovascular diseases [70].

3.2.5. Wound-healing activity

To improve wound therapeutics, a core-shell chitosan-polycaprolactone (CS/PCL) composite nanofibrous scaffold that delivers ferulic acid (FA) and RES was produced [71]. Further, an *in vivo* full thickness skin wound healing assay was performed in female albino Wistar rats. The animals treated with RES-FA-containing CS/PCL nanofibrous scaffolds presented a great and fast wound closure rate compared to the control groups (saline and native CS/PCL nanofibrous scaffolds). These results were attributed to the decrease in ROS generation species by FA, and to the RES angiogenic activity. Animals treated with RES-FA-containing CS/PCL nanofibrous scaffolds displayed, not only thicker epidermis, but also the formation of hair follicles and sebaceous glands when compared to the control groups. Additionally, it was observed that a higher number of blood vessels were formed in the RES-FA-containing CS/PCL nanofibrous scaffolds treated rats. After the rat skin biopsies, an increase in collagen synthesis was observed for the RES-FA-containing CS/PCL nanofibrous scaffolds treated group, and the collagen deposition showed a tighter packing compared with the loose arrangement presented in the control groups. The co-delivery of RES-FA by nanofibrous scaffolds is, hereby, described in Poornima and collaborators study as a promising strategy in the treatment of acute and chronic wounds [71]

4. Concluding remarks and future prospects

The delivery of bioactive molecules, such as phytophenolic compounds, has been revolutionized by the application of nanotechnology. Nanocarrier-based formulations have been developed to modulate the release of these compounds and improve cell targeting, allowing the attainment of significant therapeutic plasmatic concentrations while the toxicological profile is able to be controlled. In this sense, in the past years, nanosuspensions, polymeric NPs, nanocapsules, nanofibrous scaffolds, nanoemulsions, nanoliposomes, SLNs, protein-based NPs and CDs have been planned and designed to deliver RES and improve its bioavailability and bioactivity.

Polymeric NPs have been the most extensively used nanocarriers to increase RES bioavailability and this effect has been particularly found when the NPs are administered orally in animal models. The pharmacokinetics parameters of RES rely on numerous factors, namely the animal model, the dose administered, the administration route and period of treatment. The latter is of major concern taking into account that missing data occurs in the major of reports, hampering the establishment of objective comparisons regarding the bioavailability effects between the developed nanoformulations. Besides, in the studies cited herein, nanocarriers are composed of different materials, which contributes to the exhibition of distinct physicochemical characteristics, and, in addition, the used controls of RES formulations vary depending on the study performed. Overall, the administration of different RES-loaded nanocarriers through several distinct routes (intranasal, i.p., i.v., oral, topical) extends RES plasma concentrations for longer periods and improves other pharmacokinetics parameters, presumably due to the nanocarriers' resistance to liver metabolism [3]. Nevertheless, RES conjugation with CDs and further i.v. or oral administration, when compared with polymeric NPs, *e.g.*, reveals no significant impact on RES pharmacokinetics parameters, being CDs considered a less attractive strategy to enhance RES bioavailability [54].

In terms of bioactivity, RES-loaded nanocarriers have enhanced the anti-oxidant and anti-inflammatory properties of RES, allowing the application of encapsulated RES as a potential strategy to treat inflammatory conditions, such as ICD, endotoxic shock syndrome and inflammatory bowel disease. Furthermore, the use of submicron lipid-based delivery systems, and the combination of RES with additional anti-oxidant substances might be further studied as alternative therapeutic approaches for neurodegenerative disorders. Besides, the encapsulation of RES also exhibits improvements in the phytoalexin neuroprotective and cardioprotective properties. Likewise, nanocarriers enhance the anticancer activity of RES against colon, brain, skin (melanoma), breast, ovarian and pancreatic cancers. Furthermore, it was demonstrated in an *in vivo* chick embryo chorioallantoic membrane (CAM) assay that nanoemulsions potentiate RES antiangiogenic activity, which is particularly important since the neovascularization of tumors is an important therapeutic target in cancer therapy [72]. The nanotechnology-based carriers designed for RES delivery presented herein enabled the simultaneously administration of additional bioactive molecules besides RES, such as conventional chemotherapeutic drugs [63]. Additionally, the surface of the nanocarriers may be functionalized with ligands to receptors overexpressed in cancer cells, allowing for a RES active targeted delivery and, thus, the use of lower RES concentrations [43,62]. The creation of surface functionalized nanocarriers for the co-administration of RES and additional substances with anticancer properties will certainly further enable the development of an effective targeted combinatorial anticancer therapy.

The anti-oxidant and anti-inflammatory activities of RES are potentiated when polymeric, lipid- and protein-based RES-loaded nanocarriers are orally or topically administered. The doses administered orally tend to be higher (between 15.0–20.0 mg/kg) than those administered locally (*e.g.*, by the intrarectal route), mainly due to the first-pass effect [53,56,59]. In turn, the RES-loaded nanocarriers developed to be applied on cancer therapy are essentially administered by the parenteral route (i.v. and i.p.) and a broad range of doses between 5.0–200.0 mg/kg were already considered. Interesting to note that, in contrast with colon and ovarian cancer, notably in brain cancer, low doses of RES-loaded nanocarriers are studied. Concerning the neuroprotective and cardioprotective activities, RES nanocarriers are usually administered by the parenteral route in lower doses than the ones used to study the nanocarriers' anticancer effects.

Overall, RES-loaded nanocarriers may constitute innovative approaches to the treatment and/or prevention of a wide range of diseases, displaying prominent applications in the biomedical field. Nevertheless, it is crucial to continuously address the fate of the nanocarriers' materials. Towards that aim, and clearly assuming the lack of correlation between RES *in vitro* and *in vivo* performance, further *in vivo* studies should be performed regarding the toxicity of nanotechnology-based carriers. Only thus, it will be possible to conduct larger and randomized clinical trials, and assess the real contribute that nanotechnology holds in the delivery of RES.

Conflict of interest

The authors confirm that this article content has no conflicts of interest.

Acknowledgements

This work is funded from Portugal National Funds (FCT/MCTES, Fundação para a Ciência e a Tecnologia/Ministério da Ciência, Tecnologia e Ensino Superior) through project UID/QUI/50006/2013, co-financed by European Union (FEDER under the Partnership Agreement PT2020). It was supported as well by the grants FCT PTDC/CTM-BIO/1518/2014 and FCT PTDC/BTM-MAT/30255/2017 from the

Portuguese Foundation for Science and Technology (FCT, Fundação para a Ciência e a Tecnologia) and the European Community Fund (FEDER) through the COMPETE2020 program. The authors wish to acknowledge Fundação para a Ciência e a Tecnologia (FCT), Portuguese Agency for Scientific Research, for financial support through the Research Project POCI-01-0145-FEDER-016642. Irina Pereira acknowledges the PhD research grant SFRH/BD/136892/2018 funded by FCT and Programa Operacional Capital Humano (POCH). Laura Ferreira recognizes the PhD grant PD/BDE/142964/2018 attributed by FCT and Laboratórios Basi from Drugs R&D Doctoral Program. Mar Collado-González acknowledges a postdoctoral fellowship (grant no. 20381/PD/17) from Fundación Séneca-Agencia de Ciencia y Tecnología de la Región de Murcia (CARM).

References

[1] V. Sanna, I.A. Siddiqui, M. Sechi, H. Mukhtar, Resveratrol-loaded nanoparticles based on poly(epsilon-caprolactone) and poly(D,L-lactic-co-glycolic acid)-poly (ethylene glycol) blend for prostate cancer treatment, Mol. Pharm. 10 (2013) 3871–3881.

[2] Y.M. Tsai, W.L. Chang-Liao, C.F. Chien, L.C. Lin, T.H. Tsai, Effects of polymer molecular weight on relative oral bioavailability of curcumin, Int. J. Nanomed. 7 (2012) 2957–2966.

[3] Y.M. Tsai, C.F. Chien, L.C. Lin, T.H. Tsai, Curcumin and its nano-formulation: the kinetics of tissue distribution and blood-brain barrier penetration, Int. J. Pharm. 416 (2011) 331–338.

[4] T. Khushnud, S.A. Mousa, Potential role of naturally derived polyphenols and their nanotechnology delivery in cancer, Mol. Biotechnol. 55 (2013) 78–86.

[5] H.B. Nair, B. Sung, V.R. Yadav, R. Kannappan, M.M. Chaturvedi, B.B. Aggarwal, Delivery of anti-inflammatory nutraceuticals by nanoparticles for the prevention and treatment of cancer, Biochem. Pharmacol. 80 (2010) 1833–1843.

[6] F. Alexis, E. Pridgen, L.K. Molnar, O.C. Farokhzad, Factors affecting the clearance and biodistribution of polymeric nanoparticles, Mol. Pharm. 5 (2008) 505–515.

[7] G. Singh, R.S. Pai, Optimized PLGA nanoparticle platform for orally dosed *trans*-resveratrol with enhanced bioavailability potential, Expert Opin. Drug Deliv. 11 (2014) 647–659.

[8] S.H. Wang, C.W. Lee, A. Chiou, P.K. Wei, Size-dependent endocytosis of gold nanoparticles studied by three-dimensional mapping of plasmonic scattering images, J. Nanobiotechnol. 8 (2010) 33.

[9] J. Rejman, V. Oberle, I.S. Zuhorn, D. Hoekstra, Size-dependent internalization of particles via the pathways of clathrin-and caveolae-mediated endocytosis, Biochem. J. 377 (2004) 159–169.

[10] L. Shang, K. Nienhaus, G.U. Nienhaus, Engineered nanoparticles interacting with cells: size matters, J. Nanobiotechnol. 12 (2014) 5.

[11] S. Pasche, J. Voros, H.J. Griesser, N.D. Spencer, M. Textor, Effects of ionic strength and surface charge on protein adsorption at PEGylated surfaces, J. Phys. Chem. B 109 (2005) 17545–17552.

[12] T. Wallerath, G. Deckert, T. Ternes, H. Anderson, H. Li, K. Witte, U. Förstermann, Resveratrol, a polyphenolic phytoalexin present in red wine, enhances expression and activity of endothelial nitric oxide synthase, Circulation 106 (2002) 1652–1658.

[13] B. Catalgol, S. Batirel, Y. Taga, N.K. Ozer, Resveratrol: French paradox revisited, Front. Pharmacol. 3 (2012) 141.

[14] A.Y. Berman, R.A. Motechin, M.Y. Wiesenfeld, M.K. Holz, The therapeutic potential of resveratrol: a review of clinical trials, npg Precis. Oncol. 1 (2017) 35.

[15] H.-Y. Tsai, C.-T. Ho, Y.-K. Chen, Biological actions and molecular effects of resveratrol, pterostilbene, and 3′-hydroxypterostilbene, J. Food Drug Anal. 25 (2017) 134–147.

[16] C. Caddeo, K. Teskac, C. Sinico, J. Kristl, Effect of resveratrol incorporated in liposomes on proliferation and UV-B protection of cells, Int. J. Pharm. 363 (2008) 183–191.

[17] M. Jang, L. Cai, G.O. Udeani, K.V. Slowing, C.F. Thomas, C.W.W. Beecher, H.H.S. Fong, N.R. Farnsworth, A.D. Kinghorn, R.G. Mehta, Cancer chemopreventive activity of resveratrol, a natural product derived from grapes, Science 275 (1997) 218–220.

[18] S. Banerjee, C. Bueso-Ramos, B.B. Aggarwal, Suppression of 7, 12-dimethylbenz (a) anthracene-induced mammary carcinogenesis in rats by resveratrol: role of nuclear factor-κB, cyclooxygenase 2, and matrix metalloprotease 9, Cancer Res. 62 (2002) 4945–4954.

[19] B.B. Aggarwal, Y. Takada, O.V. Oommen, From chemoprevention to chemotherapy: common targets and common goals, Expert Opin. Investig. Drugs 13 (2004) 1327–1338.

[20] E. Pozo-Guisado, J.M. Merino, S. Mulero-Navarro, M.J. Lorenzo-Benayas, F. Centeno, A. Alvarez-Barrientos, P.M.F. Salguero, Resveratrol-induced apoptosis in MCF-7 human breast cancer cells involves a caspase-independent mechanism with downregulation of Bcl-2 and NF-κB, Int. J. Cancer 115 (2005) 74–84.

[21] V. Sanna, A.M. Roggio, S. Siliani, M. Piccinini, S. Marceddu, A. Mariani, M. Sechi, Development of novel cationic chitosan-and anionic alginate–coated poly(D,L-lactide-co-glycolide) nanoparticles for controlled release and light protection of resveratrol, Int. J. Nanomed. 7 (2012) 5501–5516.

[22] J. Gambini, M. Inglés, G. Olaso, R. Lopez-Grueso, V. Bonet-Costa, L. Gimeno-Mallench, C. Mas-Bargues, K.M. Abdelaziz, M.C. Gomez-Cabrera, J. Vina, Properties of resveratrol: *in vitro* and *in vivo* studies about metabolism, bioavailability, and biological effects in animal models and humans, Oxid. Med. Cell. Longev. 2015 (2015) 1–13.

[23] E.M. Varoni, A.F. Lo Faro, J. Sharifi-Rad, M. Iriti, Anticancer molecular mechanisms of resveratrol, Front. Nutr. 3 (2016) 8.

[24] X. Kou, N. Chen, Resveratrol as a natural autophagy regulator for prevention and treatment of Alzheimer's disease, Nutrients 9 (2017) 927.

[25] T. Szkudelski, K. Szkudelska, Resveratrol and diabetes: from animal to human studies, Biochim. et Biophys. Acta (BBA) Mol. Basis Dis. 1852 (2015) 1145–1154.

[26] T.-P. Li, W.-P. Wong, L.-C. Chen, C.-Y. Su, L.-G. Chen, D.-Z. Liu, H.-O. Ho, M.-T. Sheu, Physical and pharmacokinetic characterizations of *trans*-resveratrol (*t*-Rev) encapsulated with self-assembling lecithin-based mixed polymeric micelles (sa LMPMs), Sci. Rep. 7 (2017) 10674.

[27] A. Amri, J.C. Chaumeil, S. Sfar, C. Charrueau, Administration of resveratrol: what formulation solutions to bioavailability limitations? J. Control. Release 158 (2012) 182–193.

[28] G. Singh, R.S. Pai, *Trans*-resveratrol self-nano-emulsifying drug delivery system (SNEDDS) with enhanced bioavailability potential: optimization, pharmacokinetics and *in situ* single pass intestinal perfusion (SPIP) studies, Drug Deliv. 22 (2015) 522–530.

[29] D. Delmas, V. Aires, E. Limagne, P. Dutartre, F. Mazué, F. Ghiringhelli, N. Latruffe, Transport, stability, and biological activity of resveratrol, Ann. N. Y. Acad. Sci. 1215 (2011) 48–59.

[30] N. Pujara, S. Jambhrunkar, K.Y. Wong, M. McGuckin, A. Popat, Enhanced colloidal stability, solubility and rapid dissolution of resveratrol by nanocomplexation with soy protein isolate, J. Colloid Interface Sci. 488 (2017) 303–308.

[31] A. Francioso, P. Mastromarino, A. Masci, M. d'Erme, L. Mosca, Chemistry, stability and bioavailability of resveratrol, Med. Chem. (Los Angeles) 10 (2014) 237–245.

[32] Š. Zupančič, Z. Lavrič, J. Kristl, Stability and solubility of *trans*-resveratrol are strongly influenced by pH and temperature, Eur. J. Pharm. Biopharm. 93 (2015) 196–204.

[33] A. Burkon, V. Somoza, Quantification of free and protein-bound *trans*-resveratrol metabolites and identification of *trans*-resveratrol-C/O-conjugated diglucuronides–two novel resveratrol metabolites in human plasma, Mol. Nutr. Food Res. 52 (2008) 549–557.

[34] G. Shi, L. Rao, H. Yu, H. Xiang, H. Yang, R. Ji, Stabilization and encapsulation of photosensitive resveratrol within yeast cell, Int. J. Pharm. 349 (2008) 83–93.

[35] E. Wenzel, V. Somoza, Metabolism and bioavailability of *trans*-resveratrol, Mol. Nutr. Food Res. 49 (2005) 472–481.

[36] C.H. Cottart, V. Nivet-Antoine, C. Laguillier-Morizot, J.L. Beaudeux, Resveratrol bioavailability and toxicity in humans, Mol. Nutr. Food Res. 54 (2010) 7–16.

[37] J. Hao, Y. Gao, J. Zhao, J. Zhang, Q. Li, Z. Zhao, J. Liu, Preparation and optimization of resveratrol nanosuspensions by antisolvent precipitation using Box-Behnken design, AAPS PharmSciTech 16 (2015) 118–128.

[38] M.R. Vijayakumar, R. Kosuru, S.K. Singh, C.B. Prasad, G. Narayan, M.S. Muthu, S. Singh, Resveratrol loaded PLGA: D-α-tocopheryl polyethylene glycol 1000 succinate blend nanoparticles for brain cancer therapy, RSC Adv. 6 (2016) 74254–74268.

[39] F.Y.K. Siu, S. Ye, H. Lin, S. Li, Galactosylated PLGA nanoparticles for the oral delivery of resveratrol: enhanced bioavailability and *in vitro* anti-inflammatory activity, Int. J. Nanomed. 13 (2018) 4133–4144.

[40] S.K. Singh, V. Makadia, S. Sharma, M. Rashid, S. Shahi, P.R. Mishra, M. Wahajuddin, J.R. Gayen, Preparation and *in-vitro/in-vivo* characterization of *trans*-resveratrol nanocrystals for oral administration, Drug Deliv. Transl. Res. 7 (2017) 395–407.

[41] G. Singh, R.S. Pai, *In-vitro/in-vivo* characterization of *trans*-resveratrol-loaded nanoparticulate drug delivery system for oral administration, J. Pharm. Pharmacol. 66 (2014) 1062–1076.

[42] Y. Zu, Y. Zhang, W. Wang, X. Zhao, X. Han, K. Wang, Y. Ge, Preparation and in vitro/in vivo evaluation of resveratrol-loaded carboxymethyl chitosan nanoparticles, Drug Deliv. (2014) 1–11.

[43] L. Bu, L.C. Gan, X.Q. Guo, F.Z. Chen, Q. Song, Z. Qi, X.J. Gou, S.X. Hou, Q. Yao, *Trans*-resveratrol loaded chitosan nanoparticles modified with biotin and avidin to target hepatic carcinoma, Int. J. Pharm. 452 (2013) 355–362.

[44] S. Karthikeyan, N. Rajendra Prasad, A. Ganamani, E. Balamurugan, Anticancer activity of resveratrol-loaded gelatin nanoparticles on NCI-H460 non-small cell lung cancer cells, Biomed. Prev. Nutr. 3 (2013) 64–73.

[45] J. Hao, J. Zhao, S. Zhang, T. Tong, Q. Zhuang, K. Jin, W. Chen, H. Tang, Fabrication of an ionic-sensitive *in situ* gel loaded with resveratrol nanosuspensions intended for direct nose-to-brain delivery, Colloids Surf. B Biointerfaces 147 (2016) 376–386.

[46] V. Trotta, B. Pavan, L. Ferraro, S. Beggiato, D. Traini, L.G. Des Reis, S. Scalia, A. Dalpiaz, Brain targeting of resveratrol by nasal administration of chitosan-coated lipid microparticles, Eur. J. Pharm. Biopharm. 127 (2018) 250–259.

[47] G. Singh, R.S. Pai, *In vitro* and *in vivo* performance of supersaturable self-nanoemulsifying system of *trans*-resveratrol, Artif. Cells Nanomed. Biotechnol. 44 (2016) 510–516.

[48] F.D. Marques-Marinho, C.D. Vianna-Soares, Cellulose and its derivatives use in the pharmaceutical compounding practice, in: T. van de Ven, L. Godbout (Eds.), Cellulose - Medical, Pharmaceutical and Electronic Applications, IntechOpen, 2013.

[49] M. Zhou, X. Chen, Preparation of transdermal formulations in resveratrol nanoparticles and pharmacokinetics study, International Conference on Smart City and Systems Engineering (2016) 632–635.

[50] M.R. Vijayakumar, K.Y. Vajanthri, C.K. Balavigneswaran, S.K. Mahto, N. Mishra, M.S. Muthu, S. Singh, Pharmacokinetics, biodistribution, *in vitro* cytotoxicity and biocompatibility of Vitamin E TPGS coated *trans*-resveratrol liposomes, Colloids

Surf. B Biointerfaces 145 (2016) 479–491.
[51] D. Pandita, S. Kumar, N. Poonia, V. Lather, Solid lipid nanoparticles enhance oral bioavailability of resveratrol, a natural polyphenol, Food Res. Int. 62 (2014) 1165–1174.
[52] S. Jose, S.S. Anju, T.A. Cinu, N.A. Aleykutty, S. Thomas, E.B. Souto, *In vivo* pharmacokinetics and biodistribution of resveratrol-loaded solid lipid nanoparticles for brain delivery, Int. J. Pharm. 474 (2014) 6–13.
[53] R. Penalva, I. Esparza, E. Larraneta, C.J. Gonzalez-Navarro, C. Gamazo, J.M. Irache, Zein-based nanoparticles improve the oral bioavailability of resveratrol and its anti-inflammatory effects in a mouse model of endotoxic shock, J. Agric. Food Chem. 63 (2015) 5603–5611.
[54] S. Das, H.S. Lin, P.C. Ho, K.Y. Ng, The impact of aqueous solubility and dose on the pharmacokinetic profiles of resveratrol, Pharm. Res. 25 (2008) 2593–2600.
[55] L. Guo, Y. Peng, J. Yao, L. Sui, A. Gu, J. Wang, Anticancer activity and molecular mechanism of resveratrol-bovine serum albumin nanoparticles on subcutaneously implanted human primary ovarian carcinoma cells in nude mice, Cancer Biother. Radiopharm. 25 (2010) 471–477.
[56] C.W. Lee, F.L. Yen, H.W. Huang, T.H. Wu, H.H. Ko, W.S. Tzeng, C.C. Lin, Resveratrol nanoparticle system improves dissolution properties and enhances the hepatoprotective effect of resveratrol through antioxidant and anti-inflammatory pathways, J. Agric. Food Chem. 60 (2012) 4662–4671.
[57] R. Pangeni, S. Sharma, G. Mustafa, J. Ali, S. Baboota, Vitamin E loaded resveratrol nanoemulsion for brain targeting for the treatment of Parkinson's disease by reducing oxidative stress, Nanotechnology 25 (2014) 485102.
[58] S.N. Shrotriya, N.S. Ranpise, B.V. Vidhate, Skin targeting of resveratrol utilizing solid lipid nanoparticle-engrossed gel for chemically induced irritant contact dermatitis, Drug Deliv. Transl. Res. 7 (2017) 37–52.
[59] A.A. Lozano-Pérez, A. Rodriguez-Nogales, V. Ortiz-Cullera, F. Algieri, J. Garrido-Mesa, P. Zorrilla, M.E. Rodriguez-Cabezas, N. Garrido-Mesa, M.P. Utrilla, L. De Matteis, J.M. de la Fuente, J.L. Cenis, J. Galvez, Silk fibroin nanoparticles constitute a vector for controlled release of resveratrol in an experimental model of inflammatory bowel disease in rats, Int. J. Nanomed. 9 (2014) 4507–4520.
[60] G. Kim, C. Piao, J. Oh, M. Lee, Self-assembled polymeric micelles for combined delivery of anti-inflammatory gene and drug to the lungs by inhalation, Nanoscale 10 (2018) 8503–8514.
[61] K.H. Jung, J.H. Lee, J.W. Park, C.H. Quach, S.H. Moon, Y.S. Cho, K.H. Lee, Resveratrol-loaded polymeric nanoparticles suppress glucose metabolism and tumor growth *in vitro* and in vivo, Int. J. Pharm. 478 (2015) 251–257.
[62] W. Guo, A. Li, Z. Jia, Y. Yuan, H. Dai, H. Li, Transferrin modified PEG-PLA-resveratrol conjugates: *in vitro* and *in vivo* studies for glioma, Eur. J. Pharmacol. 718 (2013) 41–47.
[63] H. Xu, F. Jia, P.K. Singh, S. Ruan, H. Zhang, X. Li, Synergistic anti-glioma effect of a coloaded nano-drug delivery system, Int. J. Nanomed. 2017 (2017) 29–40.
[64] F. Figueiró, A. Bernardi, R.L. Frozza, T. Terroso, A. Zanotto-Filho, E.H. Jandrey, J.C. Moreira, C.G. Salbego, M.I. Edelweiss, A.R. Pohlmann, S.S. Guterres, A.M. Battastini, Resveratrol-loaded lipid-core nanocapsules treatment reduces *in vitro* and *in vivo* glioma growth, J. Biomed. Nanotechnol. 9 (2013) 516–526.
[65] B. Carletto, J. Berton, T.N. Ferreira, L.F. Dalmolin, K.S. Paludo, R.M. Mainardes, P.V. Farago, G.M. Favero, Resveratrol-loaded nanocapsules inhibit murine melanoma tumor growth, Colloids Surf. B Biointerfaces 144 (2016) 65–72.
[66] S. Jain, T. Garg, V. Kushwah, K. Thanki, A.K. Agrawal, C.P. Dora, α-Tocopherol as functional excipient for resveratrol and coenzyme Q10-loaded SNEDDS for improved bioavailability and prophylaxis of breast cancer, J. Drug Target. 25 (2017) 554–565.
[67] T. Geng, X. Zhao, M. Ma, G. Zhu, L. Yin, Resveratrol-loaded albumin nanoparticles with prolonged blood circulation and improved biocompatibility for highly effective targeted pancreatic tumor therapy, Nanoscale Res. Lett. 12 (2017) 437.
[68] R.L. Frozza, A. Bernardi, J.B. Hoppe, A.B. Meneghetti, A. Matte, A.M. Battastini, A.R. Pohlmann, S.S. Guterres, C. Salbego, Neuroprotective effects of resveratrol against Aβ administration in rats are improved by lipid-core nanocapsules, Mol. Neurobiol. 47 (2013) 1066–1080.
[69] V. Vingtdeux, U. Dreses-Werringloer, H. Zhao, P. Davies, P. Marambaud, Therapeutic potential of resveratrol in Alzheimer's disease, BMC Neurosci. 9 (2008) S6.
[70] C.F. Hung, J.K. Chen, M.H. Liao, H.M. Lo, J.Y. Fang, Development and evaluation of emulsion-liposome blends for resveratrol delivery, J. Nanosci. Nanotechnol. 6 (2006) 2950–2958.
[71] B. Poornima, P.S. Korrapati, Fabrication of chitosan-polycaprolactone composite nanofibrous scaffold for simultaneous delivery of ferulic acid and resveratrol, Carbohydr. Polym. 157 (2017) 1741–1749.
[72] S. Pund, R. Thakur, U. More, A. Joshi, Lipid based nanoemulsifying resveratrol for improved physicochemical characteristics, *in vitro* cytotoxicity and *in vivo* anti-angiogenic efficacy, Colloids Surf. B Biointerfaces 120 (2014) 110–117.